Journal Pre-proof

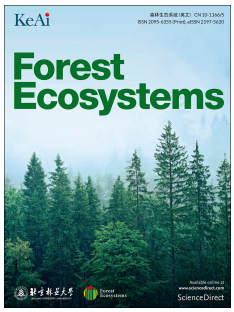

Modeling the effect of stand and site characteristics on the probability of mistletoe infestation in Scots pine stands using remote sensing data

Luiza Tymińska-Czabańska, Piotr Janiec, Paweł Hawryło, Jacek Ślopek, Anna Zielonka, Paweł Netzel, Daniel Janczyk, Jarosław Socha

PII: S2197-5620(24)00027-7

DOI: https://doi.org/10.1016/j.fecs.2024.100191

Reference: FECS 100191

To appear in: *Forest Ecosystems*

Received Date: 3 January 2024

Revised Date: 26 March 2024

Accepted Date: 26 March 2024

Please cite this article as: Tymińska-Czabańska, L., Janiec, P., Hawryło, Paweł., Ślopek, J., Zielonka, A., Netzel, Paweł., Janczyk, D., Socha, Jarosł., Modeling the effect of stand and site characteristics on the probability of mistletoe infestation in Scots pine stands using remote sensing data, *Forest Ecosystems* (2024), doi: https://doi.org/10.1016/j.fecs.2024.100191.

Modeling the effect of stand and site characteristics on the probability of mistletoe infestation in Scots pine stands using remote sensing data

Luiza Tymińska-Czabańska[1], Piotr Janiec[1,2], Paweł Hawryło[1], Jacek Ślopek[3], Anna Zielonka[4], Paweł Netzel[1], Daniel Janczyk[5], Jarosław Socha[1]

[1] Department of Forest Resources Management, Faculty of Forestry, University of Agriculture in Krakow, Al. 29 Listopada 46, Krakow 31-425, Poland

[2] Forest Management and Geodesy Bureau, ul. Lesnikow 21, 05-090 Sekocin Stary, Poland

[3] Department of Geoinformatics and Cartography, Institute of Geography and Regional Development, Faculty of Earth Sciences and Environmental Management, University of Wroclaw, pl. Uniwersytecki 1, Wroclaw, Poland

[4] Institute of Geography and Spatial Management, Faculty of Geography & Geology, Jagiellonian University in Krakow, ul. Gronostajowa 7, 30-387, Poland

[5] Torun Regional Directorate of State Forests, ul. Adama Mickiewicza 9, 87-100 Torun, Poland

Corresponding author: Luiza Tymińska-Czabańska, Department of Forest Resources Management, Faculty of Forestry, University of Agriculture in Krakow, Al. 29 Listopada 46, Krakow 31-425, Poland

E-mail address: luiza.tyminska@urk.edu.pl

Abstract

Over the past decade, the presence of mistletoe (*Viscum album* ssp. *austriacum*) in Scots pine stands has increased in many European countries. Understanding the factors that influence the occurrence of mistletoe in stands is key to making appropriate forest management decisions to limit damage and prevent the spread of mistletoe in the future. Therefore, the main objective of this study was to determine the probability of mistletoe occurrence in Scots pine stands in relation to stand-related endogenous factors such as age, top height, and stand density, as well as topographic and edaphic factors. We used unmanned aerial vehicle (UAV) imagery from 2,247 stands to detect mistletoe in Scots pine stands, while majority stand and site characteristics were calculated from airborne laser scanning (ALS) data. Information on stand age

and site type from the State Forest database were also used. We found that mistletoe infestation in Scots pine stands is influenced by stand and site characteristics. We documented that the densest, tallest, and oldest stands were more susceptible to mistletoe infestation. Site type and specific microsite conditions associated with topography were also important factors driving mistletoe occurrence. In addition, climatic water balance was a significant factor in increasing the probability of mistletoe occurrence, which is important in the context of predicted temperature increases associated with climate change. Our results are important for better understanding patterns of mistletoe infestation and ecosystem functioning under climate change. In an era of climate change and technological development, the use of remote sensing methods to determine the risk of mistletoe infestation can be a very useful tool for managing forest ecosystems to maintain forest sustainability and prevent forest disturbance.

Keywords: Generalized additive models, Tree infestation, Mistletoe occurrence, ALS, UAV, Scots pine

1. Introduction

Global climate change, particularly droughts, are a substantial cause of weakening forests, making them more susceptible to pests and pathogens inducing disturbances. In Europe, mistletoe has been mainly identified as a semi-parasite found on fir and causing the mortality of deciduous roadside and parkland trees (Szmidla et al., 2019). However, the severe droughts that hit Central Europe after 2015 caused a strong spread of mistletoe in Scots pine (*Pinus sylvestris* L.) stands, which is a source of serious disturbances (Turner and Smith, 2016). Recognizing what factors influence the occurrence of mistletoe in stands is key to making appropriate forest management decisions that limit damage and prevent the spread of mistletoe in the future.

Accelerated tree mortality and serious disturbances caused by mistletoe (*Viscum album* ssp. *austriacum*) in Scots pine stands have been observed in several countries across Europe in recent decades. In Switzerland, more than half of the Scots pine stands died off locally between 1995 and 2000 in Rhone Valley in Valais (Vertui and Tagliaferro, 1998; Zweifel et al., 2012). In pine forests of southeast Germany, a 25% reduction in the basal area growth of trees associated with mistletoe has been reported (Kollas et al., 2018). In studies from the Czech Republic on *Viscum album* occurrence in pine trees, it was demonstrated that a higher degree of infestation was recorded in stands with high drought stress (Lorenc and Vele, 2022). In Poland, a strong increase in mistletoe has been documented based on data from the mistletoe identification system implemented at the State Forest Holding. The occurrence of mistletoe was found on at least 30% of the surveyed trees, giving an estimated area of 77,500 hectares of affected Scots pine stands (Szmidla et al., 2019).

Additionally, based on ICP Forest data, a continuous increase in mistletoe was found throughout the 2008–2018 period in Poland (Lech et al., 2020). The hitherto unprecedented spread of mistletoe in the Scots pine stands of Europe can be explained by the currently observed climate change (Dobbertin, 2005). On the one hand, the number of days with average temperatures above 20 °C has increased significantly over the past 20 years, allowing mistletoe to expand beyond the northeastern part of its current natural range (Walas et al., 2022; Jeffree and Jeffree, 1996). On the other hand, there has been an increase in the average temperature during the winter season, the minimum of which is one of the most important factors limiting the occurrence of mistletoe (Iversen, 1944). Therefore, the occurrence of infestations is recorded for new areas both in the mountains and outside the current range (Dobbertin, 2005; Dobbertin and Rigling, 2006). The secretion of vascin causes the berries of mistletoe to stick to branches. In Europe, bird species of the Turdidae family, such as the *Turdus viscivorus* L. and the *Turdus pilaris* L., and of the Bombycillidae family, such as the Bohemian Waxwing (*Bombycilla garrulus* L.) and the Eurasian Blackbird (*Sylvia atricapilla* L.), are considered to be the primary vectors of mistletoe (Lech et al., 2020). Moreover, the viability of Scots pine can be severely limited by high temperatures and summer rain deficiency (Kienast et al., 1987; Dobbertin et al., 2005). Thus, the intensification of severe droughts in Europe may result in increased vulnerability to biotic stresses, including susceptibility to mistletoe.

However, the nature of mistletoe occurrence in pine stands is multifactorial. Climatic conditions favoring the spread of mistletoe are crucial, as a clear correlation of the temperature of the winter months with mistletoe occurrence has been observed (Dobbertin et al., 2005), as well as the highest percentage increase in spring air temperature and a decrease in precipitation (Szmidla et al., 2019). In addition, geographical location as well as individual tree characteristics are also important factors (Lech et al., 2020). Until recently, the identification of mistletoe-infested trees as well as many forest characteristics, such as tree height, height increment, and stand density, had been determined by traditional field methods. Today, remote sensing is a reliable source of information in forestry, and the use of various methods is constantly evolving (Senf et al., 2018; Senf and Seidl, 2021; Wang et al., 2019). Images with high spectral resolution are acquired by multi- and hyperspectral sensors installed on satellites, aircraft, or unmanned aerial vehicles (UAVs) such as drones. Cardil et al. (2019, 2017) suggests that UAV imagery and the products derived from it can provide a robust estimate of tree crowns with an acceptable level of accuracy and an assessment of tree defoliation. With high

spatial-resolution drone data, we can obtain accurate information on the location and extent of mistletoe spread in stands. While field measurements on permanent or temporary sample plots are usually limited to small areas, UAVs provide large-scale mistletoe occurrence data and low operational costs (Brovkina et al., 2018; Cardil et al., 2019). In addition, the damage assessment methodology used in field forest monitoring may underestimate mistletoe identification (Lech et al., 2020). This is due to the fact that mistletoe usually grows in the upper part of the canopy, this makes field observation methods greatly limited related to the scarce visibility of the upper crowns in the stand (Miraki et al., 2021). Although Scots pine is distinguished from other species by its good lower crown clearance, which makes it easier to identify larger mistletoes, ground observations of small mistletoe specimens are largely inaccurate. These limitations result in relatively small numbers of studies on mistletoe occurrence. However, thanks to measurements from airborne laser scanning (ALS), we can obtain high-accuracy forest stand characteristic data on an unprecedented scale (Wang et al., 2019; White et al., 2016). Consequently, the spectrum of variation in growth conditions can be greatly expanded with ALS measurements (Tymińska-Czabańska et al., 2022). Therefore, the fusion of ALS and UAV are reasonable alternatives to traditional inventory methods, which are time-consuming and costly, and may be subject to large errors (Lech et al., 2020; Noordermeer et al., 2018; Socha et al., 2017).

Studies on identifying mistletoe infection using UAVs have been very rare. Nonetheless, the monitoring of mistletoe patterns of abundance in relation to stand characteristics is critical to managing forests in an era of climate change and is extremely important in the context of studying ecosystem processes (Sayad et al., 2017). Currently, the ability to predict when and where extreme droughts or climate conditions favorable to mistletoe will occur is limited. Therefore, understanding how particular factors related to the stand explain patterns of mistletoe occurrence is of key importance for supporting forest management. Identifying stands susceptible to mistletoe infection can support the development of management strategies for forests threatened by pests and pathogens (Wulder et al., 2008). The use of remote sensing data for analysis at the level of stands as well as individual trees may be useful in detecting patterns of infection and can provide new knowledge.

Therefore, we undertook the development of a new effective approach for determining mistletoe occurrence patterns with significant use of UAV and ALS data. The main objective of the study was to determine the probability of mistletoe occurrence in the Scots pine stands in relation to stand-related endogenous factors. We hypothesized that the risk of mistletoe infestation is increased in the oldest, densest,

and tallest Scots pine stands (H1) and that the occurrence of mistletoe in Scots pine stands is driven by climatic water balance (CWB) (H2). We also hypothesized that susceptibility to mistletoe infestation may be influenced by site type and topography (H3). To meet our objectives, UAV images from 2,247 stands were used to detect mistletoe in Scots pine stands, whereas most of the stand and site characteristics were calculated on the basis of ALS data. The probability of mistletoe occurrence was then determined using Generalized Additive Models (GAMs).

2. Materials and methods

2.1. Study area

The study area covers four forest divisions located in the Toruń Regional Directorate of State Forests in the central part of Poland (Fig. 1). The dominant species in the study area is Scots pine, which mostly occurs in the sites of mixed coniferous forests and mixed forests. The proportion of the area covered by predominantly Scots pine stands is very high, at more than 89%. In smaller areas with higher productivity, there are single-species stands of alder, birch, beech, and oak. Plains and hills of post-glacial terrain dominate the landscape. The climate is warm and relatively dry. Annual precipitation is mostly below the average in Poland, i.e., below 600 mm. Locally, precipitation does not exceed 500 mm. In recent years, an increased occurrence of mistletoe, previously unknown, was found in the forest area selected for analysis. The area of each forest division comprises approximately 16,000 hectares. Within this area, we selected 2,247 managed stands of Scots pine, ensuring a representative range of site conditions and age classes for the analyses. One compact forest complex where Scots pine is the dominant species was selected in each forest district. All stands within these complexes have been the subject of analysis.

2.2. Data

2.2.1 UAV Images

Using remote UAV acquisition, high-resolution data on mistletoe occurrence can be efficiently acquired. UAV images were acquired during the vegetation season in 2020–2021 using DJI Matrice 210 V2 with a Zenmuse X5S optical camera. The flight was performed in the open category, the flight altitude was 120 meter above ground level, the lateral coverage was 75%, and the longitudinal coverage was 60%. UAV

142 images were acquired in the visible RGB band only with a 3 cm spatial resolution. More than 8,000 images
143 were obtained and processed into an orthophoto map using AgisoftMetashape software. Mistletoe detection
144 was based on manual point vectorization carried out in QGIS software. By changing the display parameters of
145 the RGB channels, the mistletoe was very clearly visible (Fig. 2). The high resolution of the UAV images
146 allowed a precise inventory of the mistletoe in the surveyed stands. Detected tree tops with mistletoes were
147 aggregated to each stand. The stands in which no mistletoe was identified were assigned to Group 0 ("No
148 mistletoe"), while the stands in which mistletoe was detected were assigned to Group 1 ("Mistletoe").
149
150 *2.2.2 ALS Data*
151 The ALS data for investigated Scots pine stands were obtained from the GUGiK (General Office of
152 Geodesy and Cartography) resources, which are openly accessible through the GIS website
153 (https://mapy.geoportal.gov.pl/). The average density of the acquired ALS data was 4 points·m^{-2}. To maintain
154 precision, the positioning error of the ALS data was carefully controlled and kept below 0.5 m by the GUGiK.
155 The acquisition of ALS point clouds occurred during the leaf-off conditions. This timing is particularly
156 significant for stands with deciduous undergrowth, since it enhances the accuracy of ground point classification
157 and consequently leads to more precise tree height determination. The ALS data processing was conducted
158 using algorithms from the lidR package for R (Roussel et al., 2020). For normalizing the point clouds to their
159 height above the ground, the "normalize_height" algorithm was employed. To generate the canopy height
160 model (CHM), the "p2r" algorithm was utilized. This algorithm determines the CHM value based on the
161 maximum height of a point, with the subcircle parameter set at 0.3 m. The function locate_trees was applied
162 with the following equation variables for Scots pine stands modification:
163 $$f = \text{function}\ (x)\ \{x \times 0.148 + 0.91\} \qquad (1)$$
164
165 *2.2.3 Calculations of Stand Characteristics from ALS Data*
166 The following ALS-derived variables were calculated for analyzed stands:
167 ● Top Height (TH): To mitigate edge effects, buffers were created around each forest stand as well as
168 along public and forest roads (Fig. 3b). The buffer size for each stand was set at 15 m. In the subsequent step,
169 the ALS data from the analyzed Scots pine stands were divided into grid cells measuring 10 m × 10 m. Within

each of these grid cells, the maximum CHM values (ZMAX) were determined (Fig. 3b). All pixels with a ZMAX less than 2/3 of the mean ZMAX were then filtered and removed from the calculation (Fig. 3c). Finally, TH was calculated as the mean of the ZMAX from each of these grid cells in each stand (Fig. 3d).

- Stand density: To calculate stand density, the treetops detected based on CHM within each 10 m × 10 m grid cell were used for calculation (Fig. 3a). To ensure accuracy in density calculations and avoid errors for stands covering small areas, a minimum stand area of 0.2 ha was assumed, and all stands below this threshold were excluded.
- Site index (SI): SI was calculated on the basis of the model developed by Socha (2021).

$$H_1 = H_0 \frac{{T_1}^{1.363}\left(T_0^{1.363}R+5920.904\right)}{T_0^{1.363}\left({T_1}^{1.363}R+5920.904\right)} \quad (2)$$

where

$$R = Z_0 + \left(Z_0^2 + \frac{2\times 5920.904\times H_1}{T_1^{1.363}}\right)^{0,5} \quad (2.1)$$

$$Z_0 = H_1 - 30.443 \quad (2.2)$$

H_0 is the height of stand at base age (100 years) - age T_0, and H_1 is the top height at age T_1 determined from the ALS.

2.2.4 Calculation of Topography Indexes

To characterize the topographic conditions in individual stands, we calculated a series of topographic indicators. A publicly available 1-meter raster digital elevation model (DEM) was used in the calculation of topographic indices and its hydrological derivatives. This model, created on the basis of LiDAR, is made available in the national geoportal (Geoportal, 2023) by GUGiK for the area of the whole country. These data, available in the form of raster tiles, were combined, and the mosaic thus created was then resampled to a 10 m resolution.

The 10 m layer thus created was then used to calculate the base layers of the DEM derivatives: aspect and slope layers. In addition, the planar (horizontal) curvature—the planC index (Wood, 1996)—was also determined using the DEM. This indicator can be calculated for areas of different size around the central raster

cell. For the purposes of this work, it was calculated for surroundings of 3 × 3, 5 × 5, 7 × 7, and 9 × 9 pixel sizes (30 × 30, 50 × 50, 70 × 70, and 90 × 90 m, respectively).

A raster layer containing the location of elementary catchments, prepared on the basis of the MPHP (Hydrographic Division Map of Poland), was used to calculate hydrological parameters. An MPHP map was developed within the framework of the project ISOK (Informatic System of National Protection against Extraordinary Hazards) as part of the implementation of the INSPIRE directive and is available within the national hydroportal (ISOK Hydroportal, 2023). For each elemental catchment present on the aforementioned map, the following layers were calculated using the 10 m DEM: local microcatchments, (potential) streams, runoff accumulation, runoff directions, and distance from streams.

During the preparation and processing of input layers, GRASS GIS (GRASS GIS, 2023) open source software modules were used: r.watershed (TWI, DTW layers) (GRASS GIS, 2023a), r.param.scale (planC, aspect and slope layers) (GRASS GIS, 2023b), r.stream.distance (EAS layer) (GRASS GIS, 2023c), r.neighbors (RTP layer) (GRASS GIS, 2023d), r.cost (DTW layer) (GRASS GIS, 2023e), and r.mapcalc (DTW layer) (GRASS GIS, 2023f). The plMapcalc (Netzel and Slopek, 2021) raster map calculator was also used because of the capabilities it has in working with large raster datasets (RTP layer). The following indices were calculated:

- RTP – Relative Topographic Position

RTP is an index of the topographic position of a selected raster cell relative to its surroundings, taking into account the spatial distribution of heights in the surroundings. It is calculated for an area of a certain size taking into account the maximum, minimum, and average height calculated for that area. The value of the index is assigned to the area's central raster cell. RTP was calculated according to the method proposed by Newman et al. (2018), for 7 × 7, 11 × 11, and 21 × 21 pixel surrounds (70 × 70, 110 × 110, and 210 × 210 m, respectively).

- TWI – Topographic Wetness Index

The TWI index, introduced by Beven and Kirkby (1979), reflects the tendency of water to accumulate at specific points in a catchment and the effect of gravity on runoff to downstream areas (Quinn et al., 1991). It is defined as the relationship between the size of the area involved in surface runoff through the study catchment point and its slope. The index values can be used for analyses of the spatial distribution of soil

moisture (the degree of moisture saturation of the land surface). The index is calculated according to Formula (3).

$$\mathrm{TWI} = \log_{\mathrm{e}}\left(\frac{\alpha}{\tan(\beta)}\right) \quad (3)$$

where α is the area feeding the runoff for the point under analysis, and β is the value of the local slope angle. The TWI index takes negative values when $\frac{\alpha}{\tan(\beta)} < 1$.

- DTW – Depth To Water

The DTW index can be used for predicting soil moisture. It is calculated based on layers of (potential) streams and the DEM (Murphy et al., 2008). The DTW values are calculated along the least-cost path, construed as the distance both vertically and horizontally from the analyzed raster cell to the nearest cell representing water (stream channel). DTW takes the value 0 for cells representing streams and increases for cells located further and higher from the stream cells. Higher values of the DTW indicate greater dryness of the area. DTW is calculated using Formula (4).

$$\mathrm{DTW} = (\sum \tan(\beta) \times \mathrm{a}) \times x_{\mathrm{c}} \quad (4)$$

where tan(β) is the tangent of the slope between successive rasters of the least-cost path determined between the analyzed raster and the stream cell; a is a constant, which takes the value of 1 if the next raster in the least-cost path is in the direction parallel to the sides of the raster cell, or √2 if the next raster is on the diagonal of the least-cost path cell; x_c is the resolution of the raster cell (in this study: 10 m).

- EAS – Elevation Above Stream

The values of the EAS index are calculated from the stream layer for local (micro) catchments and the DEM (Rennó et al., 2008). EAS is calculated as the difference in elevation between the analyzed raster cell and the nearest stream cell. When calculating distances to stream cells, runoff paths to the analyzed cells are taken into account. With use of the DEM layer, the (potential) stream layer and runoff direction layer were determined. Based on these, a resultant layer of EAS was calculated, determining the difference in elevation between the analyzed raster cell and the nearest cell defined as a (potential) stream.

All topography indexes were spatially averaged for the individual forest stands.

2.2.5 Stand Characteristics form Forest Data Bank

Forest Data Bank data were obtained for 2021 and used in the study as possible explanatory variables for mistletoe occurrence in infested stands. Data on site type, species composition, and stand age were used for the analysis.

2.2.6 Climatic Water Balance

The Climatic Water Balance (CWB) was adopted to describe water and climate conditions. To be independent of systematic errors in the measurement of precipitation and the method of calculating potential evapotranspiration, the Standardized Climatic Water Balance (SCWB) was also calculated (Łabędzki and Bąk, 2004).

The input data for the evaluation of the CWB were the spatial distributions of monthly mean air temperature (*T*) and monthly total precipitation (*R*). The spatial distributions of *T* and *R* were interpolated with a spatial resolution of 100 m for the study area for individual months from 2015 to 2019, prior to UAV data acquisition, when severe droughts were observed in the area. Public data from the Institute of Meteorology and Water Management from climate and precipitation stations were used for interpolation. The solution proposed by Thornthwaite (Pascual-Ferrer and Candela, 2015; Thornthwaite and Wilm, 1944) was adopted as the method for calculating potential evapotranspiration. This solution uses only information about average air temperature and latitude.

The CWB for the month was calculated as follows:

$$\mathrm{CWB} = R_{\mathrm{sum}} - \mathrm{ET_{th}}0 \qquad (5)$$

where CWB is climatic water balance, R_{sum} is monthly precipitation, and $\mathrm{ET_{th}}0$ is potential evapotranspiration.

The SCWB was calculated for each 100 m × 100 m grid cell using the following Formula (6).

$$\mathrm{SCWB} = \frac{\mathrm{CWB} - \mathrm{AVG_{cwb70}}}{\mathrm{STD_{cwb70}}} \qquad (6)$$

where SCWB is the standardized climatic water balance, CWB is the climatic water balance, $\mathrm{AVG}_{\mathrm{cwb70}}$ is the multi-year average of CWB for the period 1951–2022, and $\mathrm{STD}_{\mathrm{cwb70}}$ is the multi-year standard deviation of CWB for the period 1951–2022.

The CWB and SCWB were spatially averaged for the individual forest stands.

2.3 Statistical analyses and model development

In order to make a preliminary comparison of the distribution of the data in the groups of stands with and without mistletoe, the estimation of the density of the distribution for each variable was assessed using a density plot. Next, the model for the occurrence of mistletoe probability was constructed using the logistic model, which is part of the Generalized Additive Model (GAM) family (Hastie and Tibshirani, 1990). Generalized Additive Models are flexible and powerful statistical modeling techniques used for analyzing complex relationships between response variables and multiple explanatory variables. The key idea behind GAMs is to model the relationship between the response variable and each explanatory variable separately, using smooth functions, and then combine them additively. This allows for non-linear relationships between the variables to be captured, making GAMs suitable for handling data with complex and non-linear structures. The general form of a GAM is as follows:

$$g\big(E(Y)\big) = \beta_0 + f_1(x_1) + f_2(x_2) + \cdots + f_p\big(x_p\big) \quad (7)$$

where $g(E(Y))$ is the link function (logistic) applied to the expected value of the response variable Y—the probability of mistletoe occurrence; β_0 is the intercept term; $f_1(x_1)$, $f_2(x_2)$, ..., $f_p(x_p)$ are smooth functions of the explanatory variables x_1, x_2, ..., x_p.

The main advantages of GAM models lie in their effectiveness in capturing non-linear relationships, making them suitable for a wide range of applications where linear models may not be appropriate. The separate smooth functions for each variable allow easy interpretation of their individual effects on the response variable. In addition, GAMs can handle both continuous and categorical explanatory variables, as well as interactions between variables, and by using smooth functions, GAMs can avoid overfitting compared to using higher degree polynomial terms.

To avoid collinearity between variables used in modeling, we employed the variance inflation factor (VIF), a technique commonly used to detect multicollinearity among predictors in multiple linear regression

models (Cheng et al., 2022; Murray et al., 2012). High collinearity among predictors leads to elevated VIF values. Numerous studies have indicated that a VIF value surpassing 5 signifies a concerning level of collinearity (James et al., 2013; Melnychuk et al., 2017). To calculate the VIF values, we utilized the "mgcv package" in the R program. Starting with all predictors, we computed the VIF values for each and iteratively removed the variable with the highest VIF until all remaining predictors had VIF values approximately around 5. Formula (8) was used to calculate the VIF for each variable.

$$\mathrm{VIF}_{X_J} = \frac{1}{1 - R^2_{X_J \vee X_{-J}}} \qquad (8)$$

where $R^2_{X_J \vee X_{-J}}$ is R^2 from a regression of X_J on all other predictors.

For logistic regression modeling, we categorized the data into two classes: Class 1, representing stands with mistletoe (521 stands), and Class 0, representing stands without mistletoe (1,726 stands). In the end, we chose only site and stand variables that significantly influenced the probability of mistletoe occurrence and ensured they were not redundant. The model development was conducted utilizing the R package "mgcv", with smoothness parameters selected through restricted maximum likelihood selection (Wood, 2011).

3. Results

Density plots provide valuable insight into the distribution and shape of the data, helping to understand its central tendency, spread, and potential patterns. On the basis of this preliminary analysis, we found that factors such as age, stand density, the TH of stands, and elevation above sea level showed the greatest differences in the distribution of data representing groups with and without mistletoe (Fig. 4).

After excluding redundant variables, a model of the probability of mistletoe occurrence in Scots pines stands was developed. In the final version of the model, only seven variables were used that were significant (Table 2). The model developed explained 22.3% of the deviance. We found that TH, stand age, and stand density are important predictors of mistletoe presence (Fig. 5). An important determinant of the probability of mistletoe occurrence was also the stand's TH. In lower stands (TH < 20 m), the probability of the occurrence of mistletoe was relatively low. Increasing the TH to about 27 m significantly increased the probability of mistletoe occurrence (Fig. 3a). We also found that the probability of mistletoe occurrence was lowest in young

stands (<50 years) and increased rapidly from 50 to 100 years of age (Fig. 5b). The partial probability of mistletoe occurrence was highest in stands between 100 and 120 years old.

The density of the stand was the next important factor in determining the probability of occurrence. In stands with low stand density (Fig. 5c), partial mistletoe occurrence was lowest. With increasing stand density, the probability of mistletoe occurrence increased systematically and reached its highest value in stands with a density of more than 500 trees per hectare. We documented that steeper slopes and areas with higher TWI (Fig. 6a, b) also showed an increased probability of mistletoe occurrence. A slight increase in the probability of the occurrence of mistletoe was also observed in the more elevated parts of the sites (Fig. 6c). Climatic water balance was also found to influence the probability of mistletoe occurrence. Below a CWB of –12, the probability of mistletoe occurrence increased significantly (Fig. 6d).

The probability of the presence of mistletoe was also related to the forest site type (Fig. 7). The greatest risk of mistletoe presence was in the site of fresh mixed broadleaved forest, which are the most suitable site for the Scots pine. For sites that are less appropriate for Scots pine, the risk of mistletoe occurrence was lower.

4. Discussion

By embracing remote sensing technology, present studies transcend the boundaries of traditional research methods on mistletoe occurrence. Our results underline the crucial role of stand characteristics in mistletoe occurrence in Scots pine stands. In particular, mistletoe infestations tend to occur in older and more dense stands. Moreover, the probability of mistletoe infestation increases with increasing stand TH. The significant effect of topography, site type, and CWB on the occurrence of mistletoe is also demonstrated in our study. This plural insight highlights the multi-faceted nature of the relationship between mistletoe and Scots pine and broadens our understanding of this ecological phenomenon.

The ALS data provided an up-to-date picture of the stand characteristics in the study area. Together with the UAV data, the assessment of the influence of stand characteristics on the determination of mistletoe occurrence was possible. The age of the stands proved to be the most significant predictor of mistletoe infestation probability. Previous studies on the occurrence of mistletoe have also shown that the oldest and largest (dominant) trees were most frequently infested (Kołodziejek et al., 2013; Lech et al., 2020; Pilichowski et al., 2018; Sangüesa-Barreda et al., 2012). In managed Scots pine stands, which are typically even-aged, the

355 increased presence of mistletoe in the oldest age classes and tallest stands can be attributed to several
356 interrelated factors. Firstly, mature stands have larger crowns with extensive branches, providing a more
357 favorable environment for mistletoe colonization, as suggested by Overton (1994). Secondly, older stands tend
358 to attract a higher frequency of bird visitors, as documented by Aukema and Rio (2002) and Mellado and
359 Zamora (2017), which play a key role in mistletoe dispersal. In addition, the increased occurrence of mistletoe
360 in the oldest, tallest, and densest stands may be associated with a more connected canopy, providing more
361 opportunities for mistletoe seeds to attach and grow (Reich and Hawksworth, 1991; Greenwood and Weisberg,
362 2008). Previous studies have shown that maintaining high densities to reduce light in the top layer of trees can
363 reduce mistletoe occurrence and has been suggested as a silvicultural treatment against mistletoe spread
364 (Iszkuło et al., 2020). However, we found that increasing stand density increased mistletoe occurrence. The
365 possible explanations for increasing probability of mistletoe occurrence with tree density may indicate the
366 crucial role of competition for resources between trees in the current environment. The effect of density and
367 strong competition between trees for resources, especially water, can contribute to an increased susceptibility
368 to mistletoe, especially during periods of drought. We found that the probability of mistletoe occurrence
369 increases with decreasing CWB (Fig. 5D). An important background to explain this phenomenon is that the
370 mass occurrence of mistletoe in Scots pine stands in Poland coincided with the drought observed from 2015
371 to 2020. In the past, mistletoe was economically insignificant and not considered a factor in weakening and
372 killing Scots pine (Lech et al., 2020). When trees are stressed by competition for resources such as sunlight,
373 water, and nutrients, their defenses against mistletoe invasion may be compromised (Hossain et al., 2018;
374 Jactel et al., 2012; Joseph et al., 2021). Trees produce secondary metabolites such as terpenes and phenols,
375 which are involved in defense against herbivores, pathogens, and parasites. Drought stress can increase the
376 production of these compounds (Yadav et al., 2021); however, in the case of very severe and prolonged
377 drought, trees may prioritize resource allocation to maintain basic physiological functions such as water
378 transport, cell integrity, and energy production. This leaves fewer resources for defense mechanisms, and such
379 weakened trees are more susceptible to infection by mistletoe and various pests and diseases. The weakening
380 of trees due to the synergistic effects of drought and competition may explain the observed correlation of
381 mistletoe prevalence with high stand density.

Furthermore, in older and taller trees, photoassimilates and water have to be transported over longer distances, so that during drought, the balance of non-structural carbohydrates along the tree can be disturbed (Adams et al., 2017; Hesse et al., 2021; Sevanto, 2018). The described physiological mechanisms may also explain the strongest infestation of Scots pine by mistletoe observed on fertile mixed forest sites (Fig. 7). More severe drought-induced weakening observed on the most fertile sites has been reported in studies of the drought-induced mortality of Scots pine in southern Poland (Socha et al., 2023). The importance of our findings may therefore increase with the increasing number and severity of droughts associated with climate change.

Our results show that topography also plays an important role in the mistletoe infestation of Scots pine stands. We found that certain topographic conditions can create unique microclimates that favor or inhibit mistletoe infestation (Fig. 6). This may be due to the effect of the topography on local microclimatic conditions such as temperature, humidity, and wind patterns (Rita et al., 2021). The literature on the relationship between mistletoe occurrence and topography has been scarce, but the spread of mistletoe can often be favored by specific microclimatic conditions. Mistletoe occurrence in the study area was associated with valleys, higher elevations, and steeper slopes. Several factors may be considered to explain this. The positive correlation of mistletoe incidence with TWI may look seemingly paradoxical. However, a plausible explanation for this phenomenon may be that trees in the wettest locations have relatively shallow root systems and may experience much more stress during drought than trees adapted to grow in drier locations. The more frequent occurrence of mistletoe on both slopes and hillsides, on the other hand, can be explained by the fact that mistletoe, as a light-demanding species, develops best when as much light as possible reaches the treetops (Szmidla et al., 2019; Walas et al., 2022). Such favorable light conditions are found on slopes, where more of the crown is illuminated compared to flat terrain. Additionally, mistletoe seeds are primarily spread by birds that consume the mistletoe berries. The effect of topography can impact bird behavior (Guibard et al., 2022). Certain topographic features might provide suitable perching or nesting sites for birds, facilitating mistletoe seed dispersal (Martínez del Rio et al., 2015).

One of the biggest advantages of drone-derived surveys is their ability to provide wall-to-wall data from entire forest areas. Drone-assisted mistletoe occurrence studies represent an advancement in ecological research, enhancing our understanding of the complex interactions between forest characteristics, topography, and climate. Traditionally, mistletoe occurrence studies relied on ground-based surveys (Noetzli et al., 2003;

Barbu, 2009; Idžojtić et al., 2008), which have strong limitations due to the difficulty of identifying mistletoe, especially in the early stages of its development in coniferous stands. Traditional methods may also be insufficient due to the limited monitoring area and high labor intensity. Due to the nature of mistletoe, it is crucial to detect it as early as possible in the stand in order to limit its spread, so it is advisable to use methods that give rapid and precise results over a large area (Iszkulo et al., 2020). UAV-based mistletoe detection techniques offer such opportunities. The capabilities of modern UAV technology provide an unprecedented level of detail and accuracy, offering a new dimension to the investigation of mistletoe prevalence in various ecosystems, particularly in Scots pine stands. Drones equipped with high-resolution sensors allow for the capture of precise data that was previously unavailable or expensive.

A limitation of UAV-based data collection on mistletoe occurrence is that it can be used at the forest district or regional scale, whereas analysis at the national level would be too labor-intensive and expensive. In this case, attempts should be made to assess the usefulness of remote sensing data from aerial photography and high-resolution satellite imagery. Another limitation of the research presented here is that the mistletoe data were collected at a specific point in time after a 6-year drought. It seems very likely that, if the drought had not occurred, the patterns of mistletoe occurrence would have been significantly different, and one might even expect that the mass spread of mistletoe would not have been observed. Nevertheless, the results obtained indicate a very high threat from mistletoe to drought-weakened stands. The association of increased mistletoe occurrence with drought indicates another consequence of climate change in future forest management. In addition, an important aspect in the dynamics of mistletoe occurrence may be the habitat conditions for mistletoe-dispersing birds. Taking into account the habitat requirements and biology of mistletoe-dispersing birds could contribute to a better picture of mistletoe distribution patterns. Our results are at the level of the stand. Further research using local data at individual tree level is needed to draw conclusions about individual trees.

The approach presented allows the probability of mistletoe occurrence in Scots pine stands to be determined using remote sensing data. In an era of climate change and technological development, the use of remote sensing methods to determine the risk of mistletoe infestation can be a very useful tool for managing forest ecosystems with the aim to maintain forest sustainability and prevent forest disturbance.

5. Conclusions

We found that mistletoe infestation in Scots pine stands is influenced by stand and site characteristics. We documented that the densest, tallest, and oldest stands growing on fertile sites were more susceptible to mistletoe infestation. Site type and specific microsite conditions associated with the topography were also important factors driving mistletoe occurrence. In addition, CWB was a significant factor in increasing the probability of mistletoe occurrence, which is important in the context of predicted temperature increases associated with climate change. Our results are important for better understanding patterns of mistletoe infestation and ecosystem functioning under climate change. Mistletoe is becoming a real threat to forest sustainability, so a better understanding of the drivers and factors underlying mistletoe outbreaks will help in planning for adaptation and sustainable forest management.

Declaration of Competing Interest

The authors declare that they have no known competing financial interests or personal relationships that could have appeared to influence the work reported in this paper.

References

Adams, H.D., Zeppel, M.J.B., Anderegg, W.R.L., Hartmann, H., Landhausser, S.M., Tissue, D.T., Huxman, T.E., Hudson, P.J., Franz, T.E., Allen, C.D., Anderegg, L.D.L., Barron-Gafford, G.A., Beerling, D.J., Breshears, D.D., Brodribb, T.J., Bugmann, H., Cobb, R.C., Collins, A.D., Dickman, L.T., Duan, H., Ewers, B.E., Galiano, L., Galvez, D.A., Garcia-Forner, N., Gaylord, M.L., Germino, M.J., Gessler, A., Hacke, U.G., Hakamada, R., Hector, A., Jenkins, M.W., Kane, J.M., Kolb, T.E., Law, D.J., Lewis, J.D., Limousin, J.M., Love, D.M., Macalady, A.K., Martínez-Vilalta, J., Mencuccini, M., Mitchell, P.J., Muss, J.D., O'Brien, M.J., O'Grady, A.P., Pangle, R.E., Pinkard, E.A., Piper, F.I., Plaut, J.A., Pockman, W.T., Quirk, J., Reinhardt, K., Ripullone, F., Ryan, M.G., Sala, A., Sevanto, S., Sperry, J.S., Vargas, R., Vennetier, M., Way, D.A., Xu, C., Yepez, E.A., McDowell, N.G., 2017. A multi-species synthesis of physiological mechanisms in drought induced tree mortality. Nat. Ecol. Evol. 1, 1285–1291. https://doi.org/10.1038/s41559-017-0248-x.

Aukema, J.E., Martínez del Rio, C., 2002. Where does a fruit-eating bird deposit mistletoe seeds? Seed deposition patterns and an experiment. Ecology 83, 3489–3496.

Beven, K.J., Kirkby, M.J., 1979. A physically based, variable contributing area model of basin hydrology. Hydrol. Sci.

Bull. 24 (1), 43–69. doi:10.1080/02626667909491834.

Barbu, C., 2009. Impact of mistletoe attack (*Viscum album* ssp. *abietis*) on the radial growth of silver fir. A case study in the North of Eastern Carpathians. Ann. For. Res. 52, 89–96.

Brovkina, O., Cienciala, E., Surový, P., Janata, P., 2018. Unmanned aerial vehicles (UAV) for assessment of qualitative classification of Norway spruce in temperate forest stands. Geo-Spat. Inf. Sci. 21, 12–20. https://doi.org/10.1080/10095020.2017.1416994.

Cardil, A., Otsu, K., Pla, M., Silva, C.A., Brotons, L., 2019. Quantifying pine processionary moth defoliation in a pine-oak mixed forest using unmanned aerial systems and multispectral imagery. PLoS One 14, e0213027. https://doi.org/10.1371/journal.pone.0213027.

Cardil, A., Vepakomma, U., Brotons, L., 2017. Assessing pine processionary moth defoliation using unmanned aerial systems. Forests 8 (10), 402. https://doi.org/10.3390/f8100402.

Cheng, J., Sun, J., Yao, K., Xu, M., Cao, Y., 2022. A variable selection method based on mutual information and variance inflation factor. Spectrochim. Acta A: Mol. Biomol. Spectrosc. 268, 120652. https://doi.org/10.1016/j.saa.2021.120652.

Dobbertin, M., 2005. Tree growth as indicator of tree vitality and of tree reaction to environmental stress: a review. Eur. J. Forest Res. 124, 319–333. https://doi.org/10.1007/s10342-005-0085-3.

Dobbertin, M., Rigling, A., 2006. Pine mistletoe (*Viscum album* ssp. *austriacum*) contributes to Scots pine (*Pinus sylvestris*) mortality in the Rhone valley of Switzerland. For. Pathol. 36, 309–322. https://doi.org/10.1111/j.1439-0329.2006.00457.x.

Greenwood, D.L., Weisberg, P.J., 2008. Density-dependent tree mortality in pinyon-juniper woodlands. For. Ecol. Manag. 255, 2129–2137. https://doi.org/10.1016/j.foreco.2007.12.048.

Guibard, A., Sèbe, F., Dragna, D., Ollivier, S., 2022. Influence of meteorological conditions and topography on the active space of mountain birds assessed by a wave-based sound propagation model. J. Acoust. Soc. Am. 151, 3703–3718. https://doi.org/10.1121/10.0011545.

Hastie, T.J., Tibshirani, R.J., 1990. Generalized Additive Models. Routledge, New York.

Hesse, B.D., Hartmann, H., Rötzer, T., Landhäusser, S.M., Goisser, M., Weikl, F., Pritsch, K., Grams, T.E.E., 2021. Mature beech and spruce trees under drought – Higher C investment in reproduction at the expense of whole-tree NSC stores. Environ. Exp. Bot. 191, 104615. https://doi.org/10.1016/j.envexpbot.2021.104615.

Hossain, M., Veneklaas, E.J., Hardy, G.E.S.J., Poot, P., 2018. Tree host-pathogen interactions as influenced by drought timing: Linking physiological performance, biochemical defence and disease severity. Tree Physiol. 39, 6–18.

https://doi.org/10.1093/treephys/tpy113.

Idžojtić, M., Pernar, R., Glavaš, M., Zebec, M., Diminić, D., 2008. The incidence of mistletoe (*Viscum album* ssp. *abietis*) on silver fir (*Abies alba*) in Croatia. Biologia (Bratisl) 63, 81–85. https://doi.org/10.2478/s11756-008-0014-2.

Iszkulo, G., Armatys, L., Dering, M., Ksepko, M., Tomaszewski, D., Ważna, A., Giertych, M.J., 2020. Mistletoe as a threat to the health state of coniferous forest. Sylwan 164, 226–236. https://doi.org/10.26202/sylwan.2019121.

Jactel, H., Petit, J., Desprez-Loustau, M.L., Delzon, S., Piou, D., Battisti, A., Koricheva, J., 2012. Drought effects on damage by forest insects and pathogens: A meta-analysis. Global Change Biol. 18, 267–276. https://doi.org/10.1111/j.1365-2486.2011.02512.x.

James, G., Witten, D., Hastie, T., Tibshirani, R., 2013. An Introduction to Statistical Learningw with Applications in R, 1st ed. Springer-Verlag, New York.

Joseph, J., Luster, J., Bottero, A., Buser, N., Baechli, L., Sever, K., Gessler, A., 2021. Effects of drought on nitrogen uptake and carbon dynamics in trees. Tree Physiol. 41, 927–943. https://doi.org/10.1093/treephys/tpaa146.

Kollas, C., Gutsch, M., Hommel, R., Lasch-Born, P., Suckow, F., 2018. Mistletoe-induced growth reductions at the forest stand scale. Tree Physiol. 38, 735–744. https://doi.org/10.1093/treephys/tpx150.

Kołodziejek, J., Patykowski, J., Kołodziejek, R., 2013. Distribution, frequency and host patterns of European mistletoe (*Viscum album* subsp. *album*) in the major city of Lodz, Poland. Biologia 68, 55–64. https://doi.org/10.2478/s11756-012-0128-4.

Lech, P., Zółciak, A., Hildebrand, R., 2020. Occurrence of European mistletoe (*Viscum album* L.) on forest trees in Poland and its dynamics of spread in the period 2008–2018. Forests 11, 83. https://doi.org/10.3390/f11010083.

Lorenc, F., Véle, A., 2022. Characteristics of *Pinus sylvestris* stands infected by *Viscum album* subsp. *austriacum*. Austrian J. For. Sci. 139, 31–50.

Łabędzki, L., Bąk, B., 2004. Standardized climatic water balance as drought index. Acta Agroph. 3(1), 117–124.

Martínez del Rio, C., Silva, A., Medel, R., Hourdequin, M., 2015. Seed dispersers as disease vectors: bird transmission of mistletoe seeds to plant hosts. Ecology 77, 912–921.

Mellado, A., Zamora, R., 2017. Parasites structuring ecological communities: The mistletoe footprint in Mediterranean pine forests. Funct. Ecol. 31, 2167–2176. https://doi.org/10.1111/1365-2435.12907.

Melnychuk, M.C., Peterson, E., Elliott, M., Hilborn, R., 2017. Fisheries management impacts on target species status. Proc. Natl. Acad. Sci. U.S.A. 114, 178–183. https://doi.org/10.1073/pnas.1609915114.

Miraki, M., Sohrabi, H., Fatehi, P., Kneubuehler, M., 2021. Detection of mistletoe infected trees using UAV high

spatial resolution images. J. Plant Dis. Prot. 128, 1679–1689. https://doi.org/10.1007/s41348-021-00502-6.

Murphy, P.N.C., Ogilvie, J., Castonguay, M., Zhang, C., Meng, F-R., Arp, P.A., 2008. Improving forest operations planning through high-resolution flow-channel and wet-areas mapping. Forest. Chron. 84, 568–574. https://doi.org/10.5558/tfc84568-4.

Murray, L., Nguyen, H., Lee, Y., Remmenga, M.D., Smith, D.W., 2012. Variance inflation factors in regression models with dummy variables. Conference on Applied Statistics in Agriculture, New Prairie Press, Kansas. https://doi.org/10.4148/2475-7772.1034.

Netzel, P., Slopek, J., 2021. Comparison of different implementations of a raster map calculator. Comput. Geosci. 154, 104824. https://doi.org/10.1016/j.cageo.2021.104824.

Newman, D.R., Lindsay, J.B., Cockburn, J.M.H., 2018. Evaluating metrics of local topographic position for multiscale geomorphometric analysis. Geomorphology 312, 40–50. https://doi.org/10.1016/j.geomorph.2018.04.003.

Noordermeer, L., Bollandsås, O.M., Gobakken, T., Næsset, E., 2018. Direct and indirect site index determination for Norway spruce and Scots pine using bitemporal airborne laser scanner data. For. Ecol. Manag. 428, 104–114. https://doi.org/10.1016/j.foreco.2018.06.041.

Pascual-Ferrer, J., Candela, L., 2015. Water Balance on the Central Rift Valley, in Case studies for developing globally responsible engineers. GDEE (eds.), Global Dimension in Engineering Education, Barcelona. http://gdee.eu/index.php/resources.html (accessed 15 Jannuary 2024).

Pilichowski, S., Filip, R., Kościelska, A., Zaroffe, G., Zyzniewska, A., Iszkuło, G., 2018. Influence of *Viscum album* ssp. *Austriacum* (Wiesb.) Vollm. on tree radial growth of *Pinus sylvestris* L. Sylwan 162, 452–459.

Quinn, P., Beven, K., Chevallier, P., Planchon, O., 1991. The prediction of hillslope flow paths for distributed hydrological modelling using digital elevation models. Hydrol. Process. 5(1), 59–79. https://doi.org/10.1002/hyp.3360050106.

Reich, R.W., Mielke Jr., P.W., Hawksworth, F.G., 1991. Spatial analysis of ponderosa pine trees infected with dwarf mistletoe. Can. J. Forest Res. 21, 1808–1815.

Rita, A., Bonanomi, G., Allevato, E., Borghetti, M., Cesarano, G., Mogavero, V., Rossi, S., Saulino, L., Zotti, M., Saracino, A., 2021. Topography modulates near-ground microclimate in the Mediterranean *Fagus sylvatica* treeline. Sci. Rep. 11, 8122. https://doi.org/10.1038/s41598-021-87661-6.

Roussel, J.R., Auty, D., Coops, N.C., Tompalski, P., Goodbody, T.R.H., Meador, A.S., Bourdon, J.F., de Boissieu, F., Achim, A., 2020. lidR: An R package for analysis of Airborne Laser Scanning (ALS) data. Remote Sens. Environ. 251, 112061. https://doi.org/10.1016/j.rse.2020.112061.

Sangüesa-Barreda, G., Linares, J.C., Camarero, J.J., 2012. Mistletoe effects on Scots pine decline following drought events: insights from within-tree spatial patterns, growth and carbohydrates. Tree Physiol. 32, 585–598. https://doi.org/10.1093/treephys/tps031.

Sayad, E., Boshkar, E., Gholami, S., 2017. Different role of host and habitat features in determining spatial distribution of mistletoe infection. For. Ecol. Manag. 384, 323–330. https://doi.org/10.1016/j.foreco.2016.11.012.

Senf, C., Pflugmacher, D., Zhiqiang, Y., Sebald, J., Knorn, J., Neumann, M., Hostert, P., Seidl, R., 2018. Canopy mortality has doubled in Europe's temperate forests over the last three decades. Nat. Commun. 9, 4978. https://doi.org/10.1038/s41467-018-07539-6.

Senf, C., Seidl, R., 2021. Mapping the forest disturbance regimes of Europe. Nat. Sustain. 4, 63–70. https://doi.org/10.1038/s41893-020-00609-y.

Sevanto, S., 2018. Drought impacts on phloem transport. Curr. Opin. Plant Biol. 43, 76–81. https://doi.org/10.1016/j.pbi.2018.01.002.

Socha, J., Hawryło, P., Tymińska-Czabańska, L., Reineking, B., Lindner, M., Netzel, P., Grabska-Szwagrzyk, E., Vallejos, R., Reyer, C.P.O., 2023. Higher site productivity and stand age enhance forest susceptibility to drought-induced mortality. Agric. For. Meteorol. 341, 109680. https://doi.org/10.1016/j.agrformet.2023.109680.

Socha, J., Pierzchalski, M., Bałazy, R., Ciesielski, M., 2017. Modelling top height growth and site index using repeated laser scanning data. For. Ecol. Manag. 406, 307–317. https://doi.org/10.1016/j.foreco.2017.09.039.

Socha, J., Tymińska-Czabańska, L., Bronisz, K., Zięba, S., Hawryło, P., 2021. Regional height growth models for Scots pine in Poland. Sci. Rep. 11, 10330. https://doi.org/10.1038/s41598-021-89826-9.

Szmidla, H., Tkaczyk, M., Plewa, R., Tarwacki, G., Sierota, Z., 2019. Impact of common mistletoe (*Viscum album* L.) on scots pine forests-A call for action. Forests 10, 847. https://doi.org/10.3390/f10100847.

Thornthwaite, C., Wilm, H., 1944. Report of the committee on transpiration and evaporation. Trans. Am. Geophys. Union 25, 686–693.

Tymińska-Czabańska, L., Hawryło, P., Socha, J., 2022. Assessment of the effect of stand density on the height growth of Scots pine using repeated ALS data. Int. J. Appl. Earth Obs. Geoinfor. 108, 102763. https://doi.org/10.1016/j.jag.2022.102763.

Vertui, F., Tagliaferro, F., 1998. Scots pine (*Pinus sylverstris* L.) die-back by unknown causes in the Aosta Valley, Italy. Chemosphere 36, 1061–1065. https://doi.org/10.1016/S0045-6535(97)10172-2.

Walas, Ł., Kędziora, W., Ksepko, M., Rabska, M., Tomaszewski, D., Thomas, P.A., Wójcik, R., Iszkuło, G., 2022. The

587 future of *Viscum album* L. in Europe will be shaped by temperature and host availability. Sci. Rep. 12, 17072.
588 https://doi.org/10.1038/s41598-022-21532-6.
589 Wang, Y., Lehtomäki, M., Liang, X., Pyörälä, J., Kukko, A., Jaakkola, A., Liu, J., Feng, Z., Chen, R., Hyyppä, J., 2019.
590 Is field-measured tree height as reliable as believed – A comparison study of tree height estimates from field
591 measurement, airborne laser scanning and terrestrial laser scanning in a boreal forest. ISPRS J. Photogramm.
592 Remote Sens. 147, 132–145. https://doi.org/10.1016/j.isprsjprs.2018.11.008.
593 White, J.C., Coops, N.C., Wulder, M.A., Vastaranta, M., Hilker, T., Tompalski, P., 2016. Remote sensing technologies
594 for enhancing forest inventories: A review. Can. J. Remote Sens. 42, 619–641.
595 https://doi.org/10.1080/07038992.2016.1207484.
596 Wood, J., 1996. The Geomorphological Characterisation of Digital Elevation Models. Dissertation, Department of
597 Geography, University of Leicester, U.K. http://hdl.handle.net/2381/34503 (accesed 2 December 2022).
598 Wood, S.N., 2011. Fast stable restricted maximum likelihood and marginal likelihood estimation of semiparametric
599 generalized linear models. J. R. Stat. Soc. Ser. B Stat. Methodol. 73, 3–36. https://doi.org/10.1111/j.1467-
600 9868.2010.00749.x.
601 Wulder, M.A., White, J.C., Coops, N.C., Butson, C.R., 2008. Multi-temporal analysis of high spatial resolution imagery
602 for disturbance monitoring. Remote Sens. Environ. 112, 2729–2740. https://doi.org/10.1016/j.rse.2008.01.010.
603 Yadav, B., Jogawat, A., Rahman, M.S., Narayan, O.P., 2021. Secondary metabolites in the drought stress tolerance of
604 crop plants: A review. Gene Rep. 23, 101040. https://doi.org/10.1016/j.genrep.2021.101040.
605 Zweifel, R., Bangerter, S., Rigling, A., Sterck, F.J., 2012. Pine and mistletoes: How to live with a leak in the water flow
606 and storage system? J. Exp. Bot. 63, 2565–2578. https://doi.org/10.1093/jxb/err432.
607
608

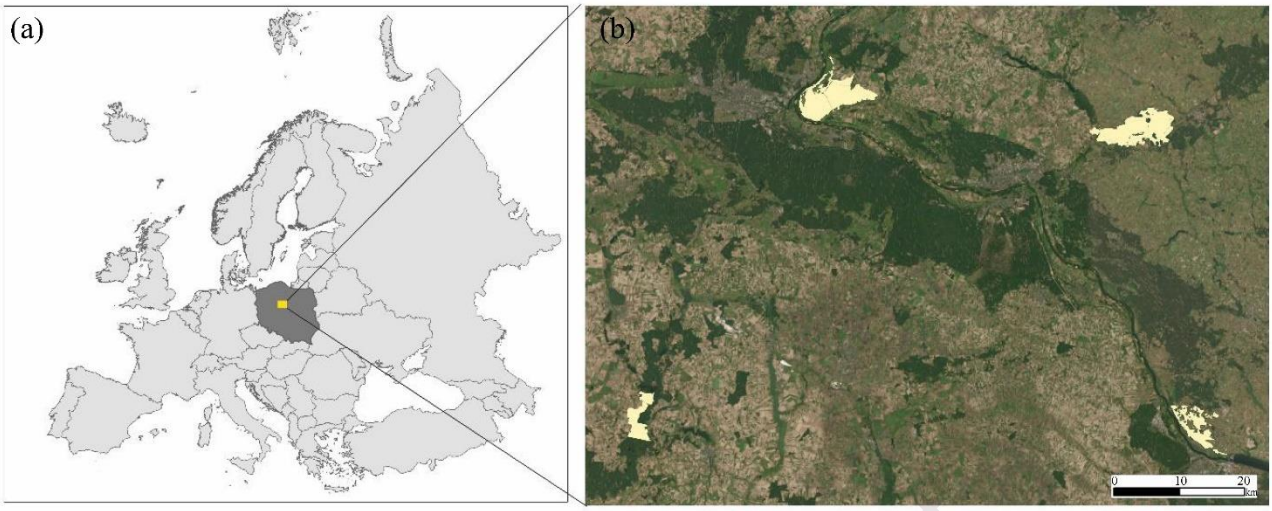

Fig. 1. Study area: (**a**) location of the study area in Europe; (**b**) location of stands covered with UAV images (light yellow color) within the Toruń Regional Directorate of State Forests.

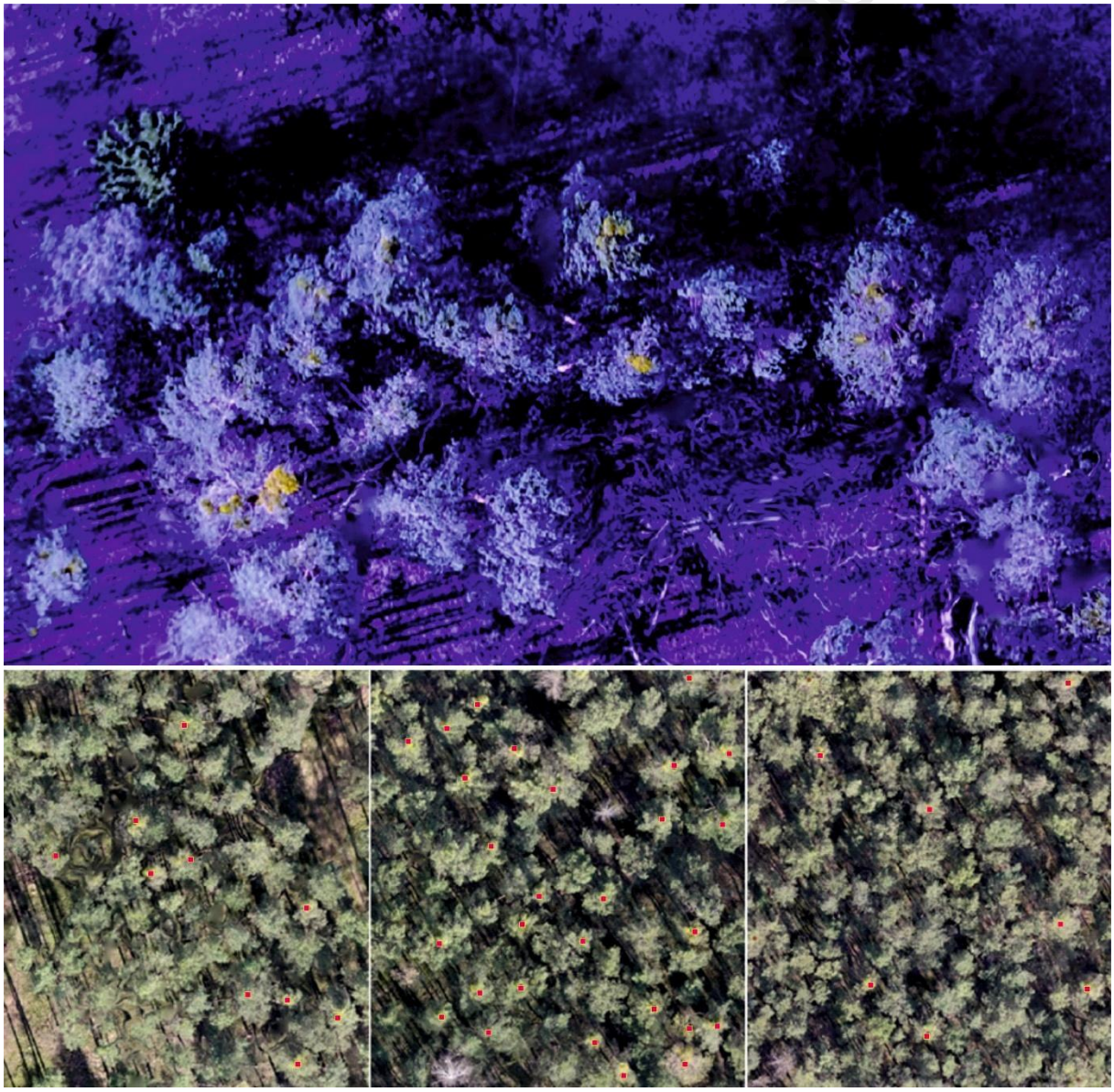

Fig. 2. UAV images from Scots pine stands infected by mistletoe. In the photo above, the RGB composite was displayed in false color to make mistletoe clearly visible. The RGB composites in natural colors in the photos below contain marked trees with mistletoe.

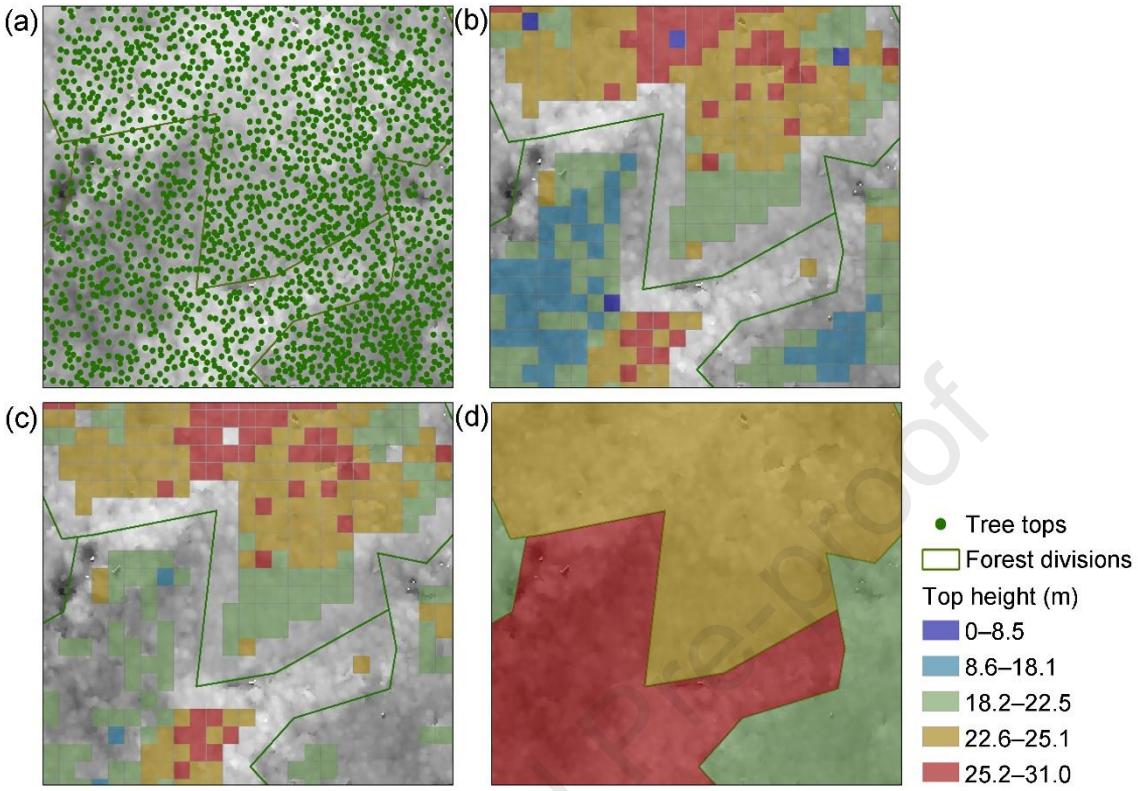

Fig. 3. Visualization of tree tops identified from ALS point cloud (**a**). The maximum CHM values (ZMAX) were determined within a designated 10 m × 10 m grid cell (**b**), and buffers created around forest divisions are marked in grey. Filtered pixels with a ZMAX less than 2/3 of the mean ZMAX (**c**). TH is calculated as the mean of the ZMAX in each stand (**d**).

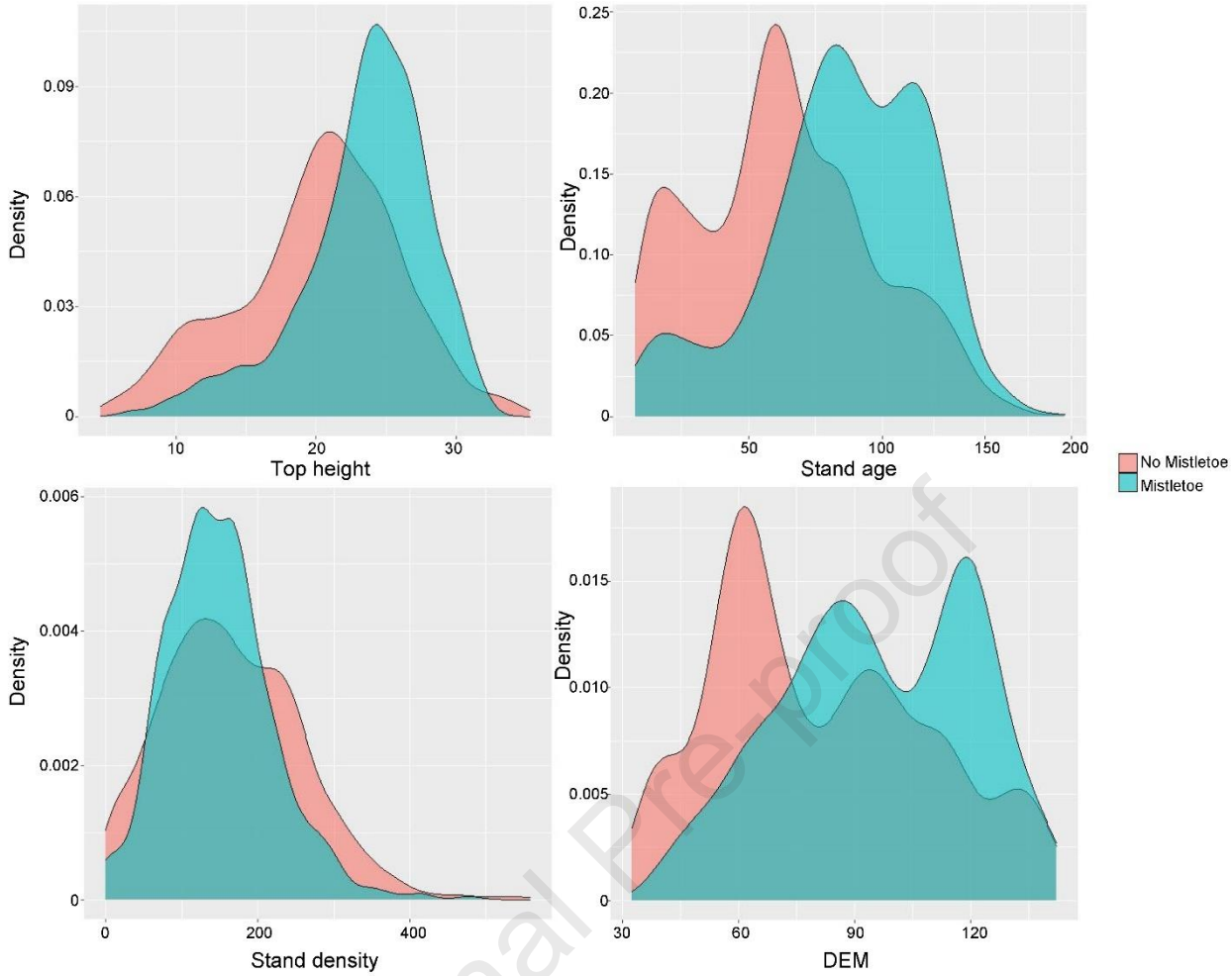

Fig. 4. Distribution of data representing groups with and without mistletoe for top height, stand age, stand density, and DEM, that showed the greatest diversity in data distribution. Orange and blue indicate stands without and with mistletoe, respectively.

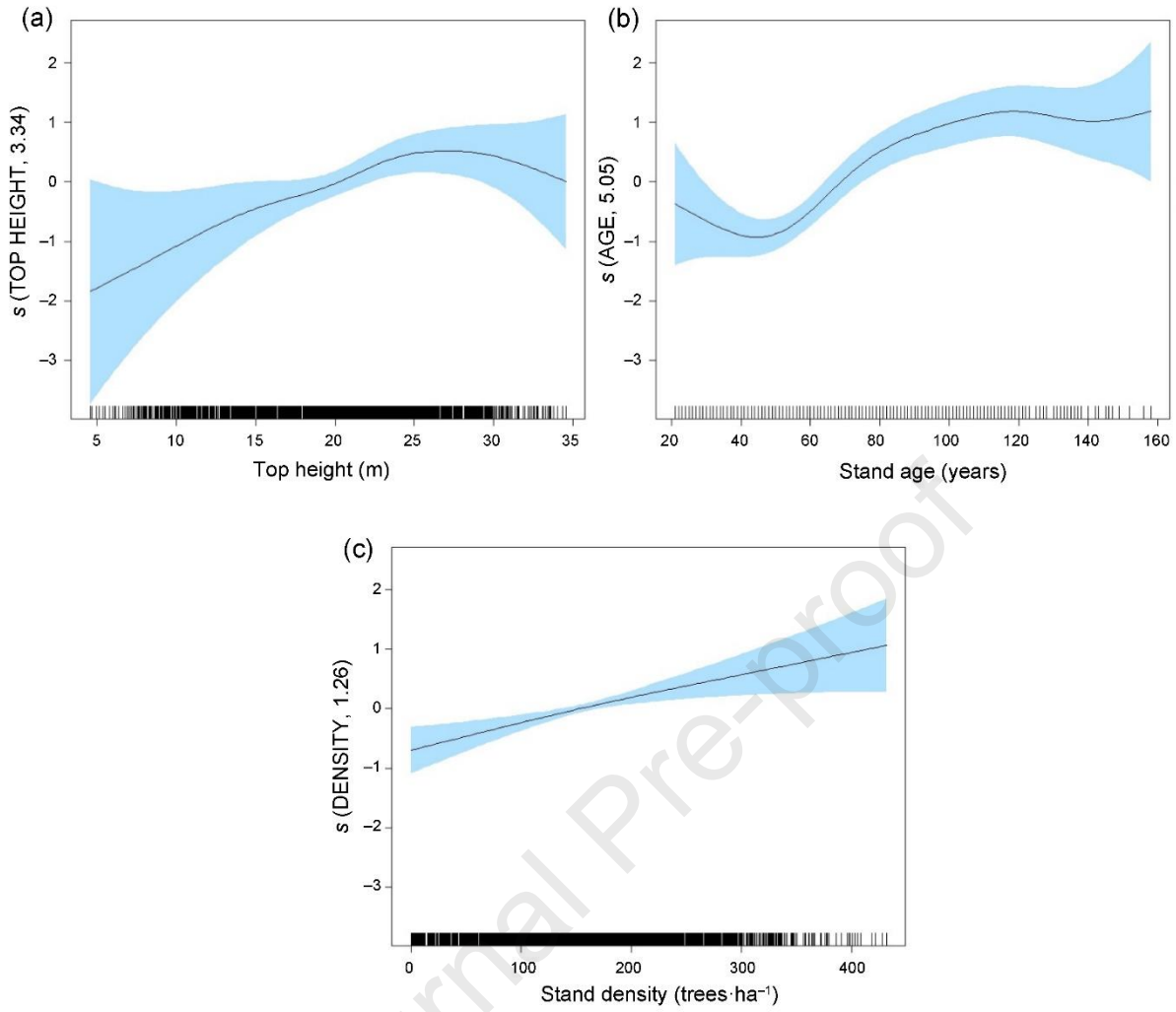

Fig. 5. Partial effects of top height (**a**), stand age (**b**), and stand density (**c**) on the probability of mistletoe occurrence at the stand level. The blue area indicates 95% confidence interval for the spline function of the GAM model (black line).

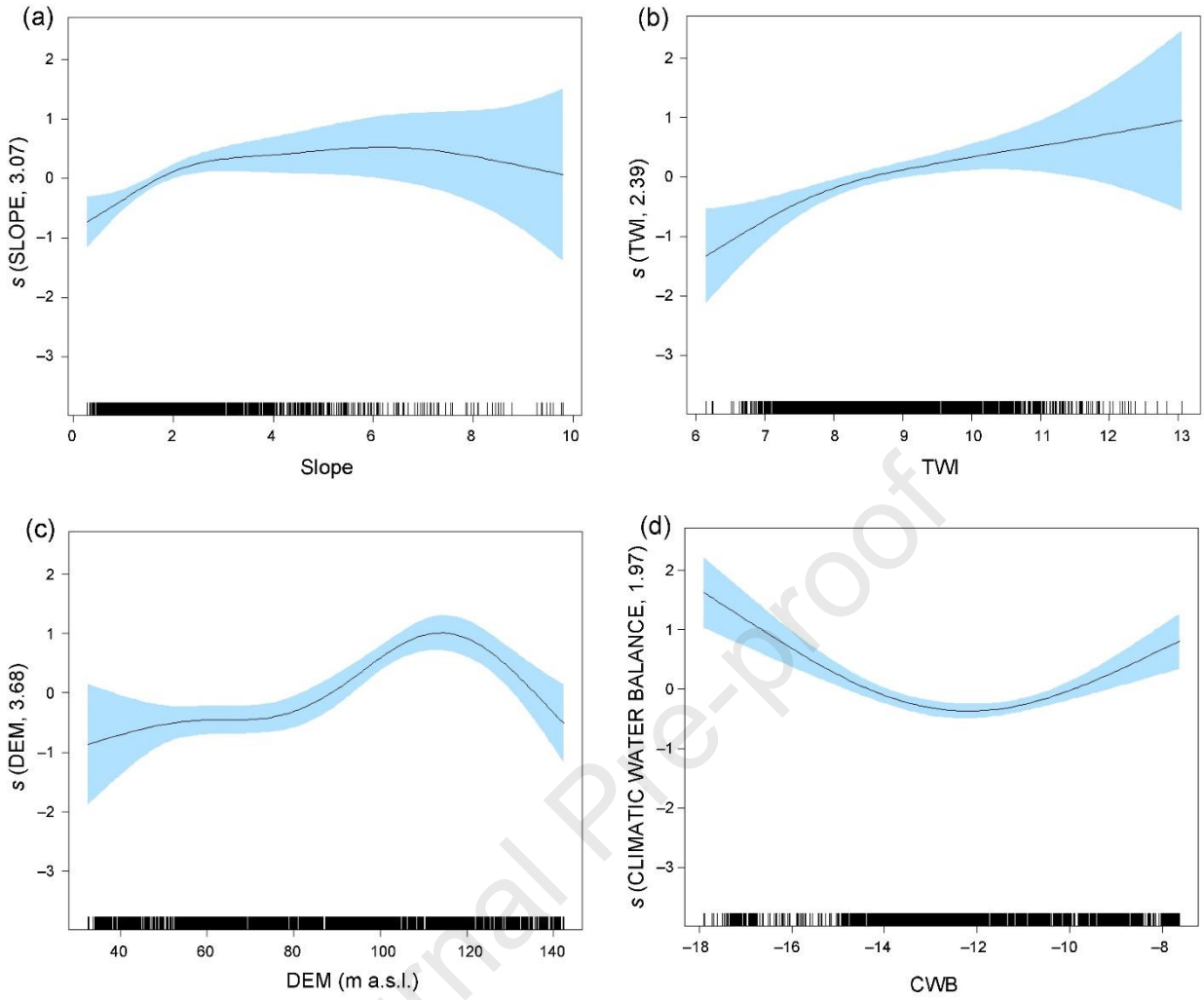

Fig. 6. Partial effects of slope (**a**), topographic wetness index (**b**, TWI), elevation above sea level (**c**, DEM), and climatic water balance (**d**, CWB) on the stand-level occurrence of mistletoe probability. The blue area indicates a 95% confidence interval for the spline function of the GAM model (black line).

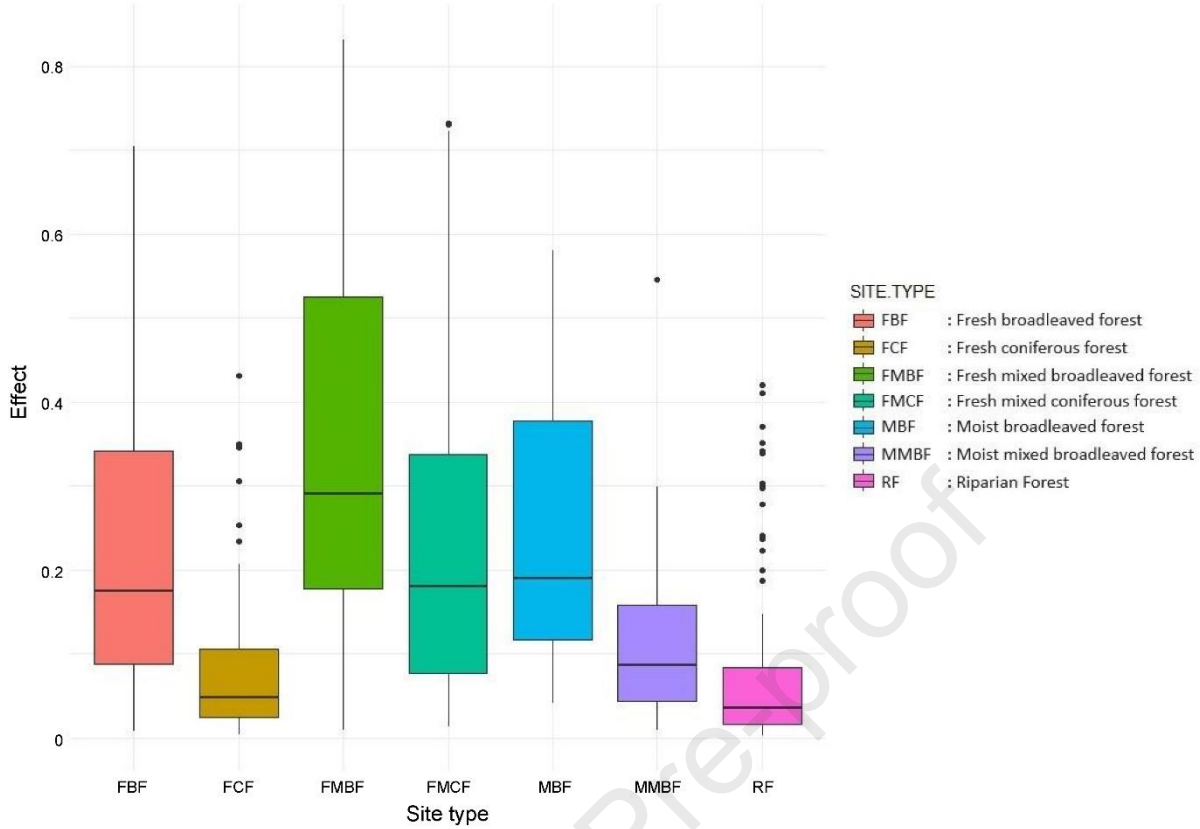

Fig. 7. Partial effects of site type on the stand-level occurrence of mistletoe probability.

638
639 **Table 1.** General characteristics of analyzed stands (yellow color from Fig. 1).

Forest divisions	Number of stands	Age (year)			Top height (m)			Occurrence of mistletoe in mistletoe-infected stands (number of trees in stands with mistletoe)	
		min	max	mean	min	max	mean	min	max
Gołąbki (both subareas)	566	21	145	72	2.0	34.34	21.95	1	177
Golub-Dobrzyń	356	21	185	71	2.6	34.34	23.21	1	228
Toruń	853	21	196	69	9.9	35.31	20.05	1	518
Włocławek	472	22	158	70	2.0	33.15	19.47	1	276

640
641
642 **Table 2.** Approximate significance of smooth terms for variables used the GAM model describing the stand-level
643 occurrence of mistletoe probability.

Variable	Equivalent degrees of freedom	Reference degrees of freedom	Chi-sq	*p*-value
TH	3.339	4.265	10.46	<0.04
Age	5.054	6.190	67.00	<0.0001
Stand density	1.262	1.484	11.50	<0.001
Mean DEM	3.679	3.939	55.72	<0.0001
Mean slope	3.069	3.849	17.02	<0.001
Mean TWI	2.386	3.055	16.70	<0.0001
Mean CWB	1.973	1.998	38.31	<0.0001

644
645
646

Highlights

- ALS and UAV data allow for assessing the probability of mistletoe occurrence;
- The densest, tallest, and oldest stands were more susceptible to mistletoe infestation;
- Site type, topography, and CWB were also important factors driving mistletoe occurrence

Declaration of interests

☒ The authors declare that they have no known competing financial interests or personal relationships
that could have appeared to influence the work reported in this paper.

☐ The authors declare the following financial interests/personal relationships which may be considered
as potential competing interests: